



Transient-thermoelastic analysis of periodically rotated functionally graded hollow cylinder

Durmuş Yarımpaç 

Received: 4 February 2021 / Accepted: 30 April 2021 / Published online: 1 June 2021
© The Author(s), under exclusive licence to Springer Nature B.V. 2021

Abstract A closed-form solution for transient thermal stress analysis of functionally graded hollow cylinder exposed to high-temperature difference is obtained under the influence of periodic rotation. All mechanical and thermal properties except the Poisson's ratio are assumed to be graded in the radial direction as a power-law function. The transient heat conduction and equilibrium equations are solved on the Laplace domain by using Bessel functions and the Gauss quadrature integration procedure. The inverse transformation to the real space is achieved by using the modified Durbin method. The novelty of this study is to provide a general solution to the functionally graded cylinder under the effect of periodic rotation in a transient regime. The effects of periodic rotation and high-temperature difference on temperature and thermal stresses are investigated for a specific ceramic-metal mixture by using this solution. The solution presented in this study can be adopted simply by changing the coefficients of inhomogeneity in the power-law variation for any pair of materials.

Keywords Closed-form solution · Functionally graded materials · Hollow thick-walled cylinder · Periodic rotation · Transient thermal stress analysis

1 Introduction

Structural elements rotating around their longitudinal axes are used in various fields of industry. These elements are found in engines, gearboxes, steam, gas and wind turbines, helicopter blades, and tools such as cutters used in drilling and milling operations. These components, found in many devices and equipment, are subjected to constant stresses and mechanical and/or thermal loads that can cause deformation. How to minimize the effects on these rotating components is an essential issue in engineering. Therefore, these rotary elements have to be manufactured at the highest quality to be safe and durable in the long term. Functionally graded materials shown as an alternative to composite materials [1] have been under scrutiny and researched by scientists. It represents a class of materials in which mechanical and thermal properties are continually changing macroscopically throughout the entire volume. Although its production (see, e.g., [2,3] for processing techniques) is more complex and costly than composite materials, it is a popular subject because it can eliminate and/or control thermal stresses in structural components. This new class of material, which was created for the first time by Japanese scientists [4] to produce a heat-resistant

D. Yarımpaç (✉)
Department of Mathematics, Osmaniye Korkut Ata University, Osmaniye, Turkey
e-mail: durmusyarimpac@osmaniye.edu.tr

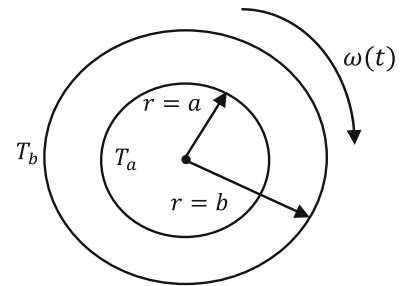
plate, has applications in many different fields such as military and aerospace industries, mechanical structural elements, prosthesis, and dental implants. For this reason, there are dozens of studies on the rotation of functionally graded structural elements subjected to thermal and/or mechanical loads in transient and steady regimes at a constant angular velocity. In this article, rather than a comprehensive literature review, a brief discussion will be given about recent research on this subject.

There are many studies in the literature on the rotation of functionally graded structure elements with a constant angular velocity. Purely elastic, partially plastic, and fully plastic deformation behavior of rotated functionally graded hollow shafts are presented analytically by Akis and Eraslan [5]. A closed-form solution of functionally graded rotating circular disks subjected to a constant angular velocity and uniform temperature change is presented by You et al. [6]. The exact elastic analysis of composite structures composed of three-layer sandwich solid-rotating disks with faces made of different isotropic materials and a core made of FGM are investigated in [7]. Asghari and Ghafoori [8] presented a three-dimensional elastic solution of functionally graded hollow and solid disks rotated with constant angular velocity. They generalized a two-dimensional solution to a three-dimensional one by modifying the plane-stress solution. Exact solutions using the infinitesimal theory of elasticity in a functionally graded cylindrical pressure vessel rotated with constant angular velocity are obtained under generalized plane strain, and plane stress and cylinder with closed ends [9]. Peng and Li [10] introduced a new approach to transform the thermoelastic problem of a functionally graded hollow circular rotating disk into solving a Fredholm integral equation. They used a simple Voigt rule to simulate the random variation of the radial material properties of a functionally graded hollow disk composed of two-phase composites.

Extensive investigations into the effect of angular velocity on a functionally graded piezoelectric rotary cylinder's mechanical and electrical responses are carried out analytically in [11]. Elastic analysis of a thin orthotropic functionally graded hollow circular disk rotating at constant angular speed about its axis for different grading indices is studied in [12]. An electro-thermoelastic detailed analysis of a long, radially polarized, functionally graded hollow cylinder rotating around its axis at a constant angular velocity is presented by Dai et al. [13]. The magneto-thermoelastic analysis of a functionally graded rotating disk with variable thickness under plane-stress condition is presented by Bayat et al. [14]. Nejad and Kashkoli [15] investigated the time-dependent thermoelastic creep response of isotropic rotating thick-walled functionally graded cylindrical pressure vessels subjected to a steady-state thermal loading. Hosseini and Dini [16] studied the magneto-elastic and magneto-thermoelastic analysis of a functionally graded rotating thick-walled cylinder subjected to uniform external magnetic and thermal field under plane strain conditions, separately. They observed that when the magnetic field is applied to the system alone, it has appropriate effects on the elastic response and improves them. However, when the magnetic and thermal fields are applied simultaneously, the elastic response behavior is reversed. Thermoelastic analysis of functionally graded thick variable cross-section cylindrical pressure vessels rotated with constant angular velocity subjected to the temperature gradient and non-uniform internal pressure is studied in [17]. A closed-form analytical solution for the Navier equation of the functionally graded rotating thick cylindrical pressure vessels under both plane-stress and plane-strain assumptions is presented using the Frobenius series method in [18].

Thermoelastic analysis of a functionally graded micro-cylinder rotated with a constant angular velocity is studied using a strain gradient elasticity formulation in [19]. The exact solution of transient thermoelastic analysis of a functionally graded thick cylindrical pressure vessel under arbitrary boundary and initial conditions is presented by Afshin et al. [20]. Dai and Dai [21] examined a rotating functionally graded magneto-electro-elastic circular disk with variable thickness under the thermal environment. The magneto-thermoelastic response of the functionally graded thick-walled rotating spherical pressure vessel is investigated in [22]. Torabnia et al. [23] presented an analytical solution of the elastic-plastic deformation of the functionally graded material hollow rotor under a high centrifugal effect and investigate the effects of the density on the failure of this elastic fully plastic in a hollow, rotating shaft concerning Tresca's yield criteria. Yildirim and Tutuncu [24] analyzed rotational elastic instability in heterogeneous disks of varying thickness under magnetic field and thermal load. Generalized elastic solutions of rotating pressurized axisymmetric vessels made of functionally graded materials for all geometries are presented by Kacar [25]. Lin [26] proposed a complete elastic analysis of a rotated thin-walled functionally graded circular disk using the infinitesimal theory of elasticity and axially symmetrical plane-stress assumptions. The transient

Fig. 1 The cross-section of a functionally graded cylinder under the effect of time-dependent angular velocity $\omega(t)$



thermoelastic analysis of a functionally graded cylinder rotating with a constant angular velocity is performed under first-order shear deformation theory and three-dimensional elasticity theory using finite difference and Eigenvalue-Eigenvector method in [27]. An analytical solution of elastoplastic analysis in a functionally graded thick-walled transverse isotropic cylinder under a radial temperature gradient and uniform pressure is presented using Seth's transition theory and generalized strain measurement theory [28].

Most of the previous work, some of which are presented above, has generally examined temperature distributions, deformations, stresses, and (transient) thermal stresses under the influence of a constant angular velocity. Rotating components' behavior requires a better understanding of their behavior to eliminate or even delay the occurrence of any instability that jeopardizes their life and increases their efficiency. Therefore, more work is needed in this direction as the stresses during the rotate up/down operation must be determined for the rotating structure's safety. Stress values resulting from constant rotation are not the same for varying rotation speed, so they cannot describe situations during the rotation is up and down operation [29]. Additionally, considering that these structural systems operate in harsh environmental conditions such as high temperatures, advanced structural models have to be designed to resist without catastrophic failure [30]. For this reason, the use of functionally gradient material is likely to eliminate naturally produced deficiencies instead.

In this article, unlike the literature, see, e.g., [9,11,17,18,20], a general solution to the functionally graded cylinder under the effect of periodic rotation in transient regime is presented. The effect of the inertia term is also taken into account due to the time-dependent rotation. All mechanical and thermal properties except the Poisson's ratio are assumed to be graded in the radial direction as a power-law function. These conditions result in linear partial differential equations for both transient heat conduction and thermoelastic analysis. The closed-form solutions of these equations are obtained using Bessel functions, the variation of parameters method, and Gaussian quadrature integration in the Laplace domain. The transformation from Laplace domain to time domain is achieved using a modified Durbin's method [31]. The effects of periodic rotation and high-temperature difference on temperature and thermal stresses are determined for a specific ceramic-metal mixture by using this general solution.

2 Transient-thermoelastic analysis

A long hollow functionally graded cylinder under the effect of high-temperature difference and time-dependent angular velocity $\omega(t)$ is examined. The cross-section area of the cylinder with inner radius a , outer radius b is given in Fig. 1. Thermal and mechanical properties are graded as a power-law function except Poisson's ratio, which varies in a small range in a functionally graded material. It is assumed that the thermal conductivity, density, specific heat, modulus of elasticity, and thermal expansion coefficient change with $\lambda(r) = \lambda_b(r/b)^{m_1}$, $\rho(r) = \rho_b(r/b)^{m_2}$, $c_p(r) = c_{pb}(r/b)^{m_3}$, $E(r) = E_b(r/b)^{m_4}$ and $\alpha(r) = \alpha_b(r/b)^{m_5}$ relations, respectively. Here the subscript b corresponds the properties of the outer surface, and m_i , $i = 1, 2, 3, 4, 5$ are the inhomogeneity parameters of the functionally graded material.

2.1 Transient heat conduction

Consider that a long hollow functionally graded cylinder with inner radius a , outer radius b . and initially at ambient temperature is suddenly exposed to different internal and external temperatures. Then, transient heat conduction equations [32,33] in cylindrical coordinate can be given in the following form:

$$\frac{1}{r} \frac{\partial}{\partial r} \left(r \lambda(r) \frac{\partial T}{\partial r} \right) = \rho(r) c(r) \frac{\partial T}{\partial t}. \quad (1)$$

For the sake of simplicity, transient heat conduction equation in a nondimensional form is obtained by using the material properties given in a power-law form with the dimensionless parameter: $\eta = r/b$, $\Theta = (T - T_0)/T_0$ and $\tau = (\lambda_b t)/(\rho_b c_{pb} b^2)$ as below:

$$\frac{\partial^2 \Theta}{\partial \eta^2} + \left(\frac{m_1 + 1}{\eta} \right) \frac{\partial \Theta}{\partial \eta} = \eta^{m_2 + m_3 - m_1} \frac{\partial \Theta}{\partial \tau}, \quad (2)$$

with a nondimensional initial condition and boundary conditions

$$\Theta(\eta, 0) = 0, \quad (3a)$$

$$\Theta(a/b, \tau) = \Theta_a, \quad \Theta(1, \tau) = \Theta_b, \quad (3b)$$

where Θ_a and Θ_b are the nondimensional temperature at the inner and outer surface, respectively. By using the Laplace transform, time dependency of the transient heat conduction equation is eliminated and an ordinary differential equation in terms of nondimensional radial direction are obtained with nondimensional boundary conditions as follows:

$$\bar{\Theta}'' + \left(\frac{m_1 + 1}{\eta} \right) \bar{\Theta}' - \eta^{m_2 + m_3 - m_1} s \bar{\Theta} = 0, \quad (4)$$

$$\bar{\Theta}(a/b, s) = \Theta_a/s, \quad \bar{\Theta}(1, s) = \Theta_b/s. \quad (5)$$

Here, $\bar{\Theta}(\eta, s) = \mathcal{L}[\Theta(\eta, \tau)]$, s is the Laplace parameter and $()'$ shows the derivative corresponding to η . The solution of the transient heat conduction equation (4) in Laplace space is

$$\bar{\Theta} = \eta^{\psi_1} [A J_{\phi_1}(\beta_1 \eta^{\gamma_1}) + B Y_{\phi_1}(\beta_1 \eta^{\gamma_1})], \quad (6)$$

where J_{ϕ_1} and Y_{ϕ_1} correspond to the first and second kinds of the Bessel functions, respectively, and

$$\psi_1 = -\frac{m_1}{2}, \quad \gamma_1 = \frac{m_2 + m_3 - m_1 + 2}{2}, \quad \phi_1 = \sqrt{\frac{\psi_1^2}{\gamma_1^2}}, \quad \beta_1 = \sqrt{\frac{-s}{\gamma_1^2}}.$$

Integration constants A and B are derived from the boundary conditions (5) as follows:

$$A = \frac{\Theta_a/s Y_{\phi_1}(\beta_1) - \Theta_b/s R^{\psi_1} Y_{\phi_1}(\beta_1 R^{\gamma_1})}{R^{\psi_1} J_{\phi_1}(\beta_1 R^{\gamma_1}) Y_{\phi_1}(\beta_1) - R^{\psi_1} Y_{\phi_1}(\beta_1 R^{\gamma_1}) J_{\phi_1}(\beta_1)},$$

$$B = \frac{\Theta_b/s R^{\psi_1} J_{\phi_1}(\beta_1 R^{\gamma_1}) - \Theta_a/s J_{\phi_1}(\beta_1)}{R^{\psi_1} J_{\phi_1}(\beta_1 R^{\gamma_1}) Y_{\phi_1}(\beta_1) - R^{\psi_1} Y_{\phi_1}(\beta_1 R^{\gamma_1}) J_{\phi_1}(\beta_1)}.$$

The transformation of the temperature field from the Laplace domain to the time domain is obtained using the modified Durbin's method [31].

2.2 Thermoelastic formulation

Consider the transient thermoelasticity of a functionally graded hollow cylinder rotated by a periodic angular velocity, $\omega(t)$. The periodic rotation of the cylinder is assumed to be slowly accelerated, so the dynamic effect

resulting from this rotation is small enough to be negligible. Under the plane strain and axisymmetry assumptions, the governing equations, initial and boundary conditions of a hollow cylinder consist of [34,35]

Strain displacement relations:

$$\epsilon_r = \frac{\partial u}{\partial r}, \quad \epsilon_\theta = \frac{u}{r}. \tag{7}$$

Constitutive relations:

$$\sigma_r = E [C_{11}\epsilon_r + C_{12}\epsilon_\theta - \alpha(C_{11} + 2C_{12})T], \tag{8a}$$

$$\sigma_\theta = E [C_{11}\epsilon_\theta + C_{12}\epsilon_r - \alpha(C_{11} + 2C_{12})T]. \tag{8b}$$

Stress equilibrium equation disregarding the body force:

$$\frac{\partial \sigma_r}{\partial r} + \frac{\sigma_r - \sigma_\theta}{r} + \rho\omega(t)^2 r = \rho \frac{\partial^2 u}{\partial t^2}, \tag{9}$$

and initial and traction-free boundary conditions:

$$u = 0 = \frac{\partial u}{\partial t} \quad \text{at } \tau = 0, \tag{10a}$$

$$\sigma_r = 0 \quad \text{at } r = a, b, \tag{10b}$$

with

$$C_{11} = \frac{1 - \nu}{(1 + \nu)(1 - 2\nu)}, \quad C_{12} = \frac{\nu}{(1 + \nu)(1 - 2\nu)}.$$

Putting equations (7) and (8) into the equilibrium Eq. (9) together with the modulus of elasticity, and the linear thermal expansion coefficient given in power-law form and using the dimensionless variables $U = u/b$, $W = \sqrt{\rho_b \omega^2 b^2 / E_b}$ and $\kappa = \lambda_b / (\rho_b c_{pb})$, a partial differential equation in terms of nondimensional radial displacement can be written as follows:

$$\begin{aligned} &\frac{\partial^2 U}{\partial \eta^2} + \left(\frac{m_4 + 1}{\eta}\right) \frac{\partial U}{\partial \eta} + \left(\frac{m_4 V_1 - 1}{\eta^2}\right) U + \frac{W^2}{C_{11}} \eta^{m_2 - m_4 + 1} \\ &= \eta^{m_2 - m_4} \frac{\rho_b \kappa^2}{E_b C_{11} b^2} \frac{\partial^2 U}{\partial \tau^2} + \alpha_b T_b V_2 \eta^{m_5} \left[\frac{\partial \Theta}{\partial \eta} + \frac{m_4 + m_5}{\eta} (\Theta + 1) \right]. \end{aligned} \tag{11}$$

Taking the Laplace transform with given initial conditions (10a), time dependency of the displacement Eq. (11) is eliminated and an ordinary differential equation is obtained in Laplace space as follows:

$$\begin{aligned} &\overline{U}'' + \left(\frac{m_4 + 1}{\eta}\right) \overline{U}' + \left(\frac{m_4 V_1 - 1}{\eta^2} - \eta^{m_2 - m_4} \frac{\rho_b \kappa^2}{E_b C_{11} b^2} s^2\right) \overline{U}' \\ &= -\frac{\overline{W}^2}{C_{11}} \eta^{m_2 - m_4 + 1} + \alpha_b T_b V_2 \eta^{m_5} \left[\overline{\Theta}' + \frac{m_4 + m_5}{\eta} \left(\overline{\Theta} + \frac{1}{s}\right) \right], \end{aligned} \tag{12}$$

with boundary conditions (10b) in terms of displacement in Laplace space:

$$\overline{U}' + \frac{V_1}{\eta} \overline{U} = \alpha_b T_b V_2 \eta^{m_5} \left(\overline{\Theta} + \frac{1}{s}\right) \quad \text{at } \eta = R, 1. \tag{13}$$

Here $\overline{U}(\eta, s) = \mathcal{L}[U(\eta, \tau)]$, $\overline{W}(s) = \mathcal{L}[W(\tau)]$, $V_1 = \nu/(1 - \nu)$, $V_2 = (1 + \nu)/(1 - \nu)$, $R = a/b$, and $()'$ shows the derivative with respect to η . The solution of this nonhomogeneous differential equation (12) consists homogeneous and particular solution.

$$\overline{U} = \overline{U}_h + \overline{U}_p. \tag{14}$$

The homogeneous solution of equation (12) is in the form of Bessel’s equation, so it can be written as follows:

$$\bar{U}_h = \eta^{\psi_2} [C_1 J_{\phi_2}(\beta_2 \eta^{\gamma_2}) + C_2 Y_{\phi_2}(\beta_2 \eta^{\gamma_2})], \tag{15}$$

where J_{ϕ_2} and Y_{ϕ_2} correspond to the first and second kinds of the Bessel functions, respectively, and

$$\begin{aligned} \psi_2 &= -\frac{m_4}{2}, & \gamma_2 &= \frac{m_2 - m_4 + 2}{2}, \\ \phi_2 &= \sqrt{\frac{\psi_2^2 - m_4 V_1 + 1}{\gamma_2^2}}, & \beta_2 &= \sqrt{\frac{-\rho_b \kappa^2 s^2}{E_b C_{11} b^2 \gamma_2^2}}. \end{aligned}$$

The particular solution of equation (12) can be found with the help of the variation of parameters method and written in the following form:

$$\bar{U}_p = \eta^{\psi_2} [D_1(\eta) J_{\phi_2}(\beta_2 \eta^{\gamma_2}) + D_2(\eta) Y_{\phi_2}(\beta_2 \eta^{\gamma_2})]. \tag{16}$$

Here, the variable coefficients obtained by the variation of parameters method are expressed by the following integrals:

$$D_1(\eta) = \int_R^\eta \frac{Z_1 \left(-\frac{\bar{W}^2}{C_{11}} y^{m_2 - m_4 + 1} + \alpha_b T_b V_2 y^{m_5} \left[\bar{\Theta}' + \frac{m_4 + m_5}{y} \left(\bar{\Theta} + \frac{1}{s} \right) \right] \right)}{Z_1 Z_2' - Z_1' Z_2} dy, \tag{17a}$$

$$D_2(\eta) = \int_R^\eta \frac{-Z_2 \left(-\frac{\bar{W}^2}{C_{11}} y^{m_2 - m_4 + 1} + \alpha_b T_b V_2 y^{m_5} \left[\bar{\Theta}' + \frac{m_4 + m_5}{y} \left(\bar{\Theta} + \frac{1}{s} \right) \right] \right)}{Z_1 Z_2' - Z_1' Z_2} dy, \tag{17b}$$

with

$$Z_1(\eta) = \eta^{\psi_2}(\eta) J_{\phi_2}(\beta_2 \eta^{\gamma_2}), \quad Z_2(\eta) = \eta^{\psi_2}(\eta) Y_{\phi_2}(\beta_2 \eta^{\gamma_2}).$$

These integrals (17) are calculated by using the Gauss quadrature method using four points. The integration constants C_1 and C_2 are derived from the boundary conditions (13) as follows:

$$\begin{aligned} C_1 &= \frac{Rhs(R)G_2(1) - Rhs(1)G_2(R)}{G_1(R)G_2(1) - G_2(R)G_1(1)}, \\ C_2 &= \frac{Rhs(1)G_1(R) - Rhs(R)G_1(1)}{G_1(R)G_2(1) - G_2(R)G_1(1)}. \end{aligned}$$

where

$$\begin{aligned} G_1(\eta) &= Z_1'(\eta) + \frac{V_1}{\eta} Z_1(\eta), \\ G_2(\eta) &= Z_2'(\eta) + \frac{V_1}{\eta} Z_2(\eta), \\ Rhs(\eta) &= \alpha_b \cdot T_b V_2 \eta^{m_5} \left(\bar{\Theta}(\eta) + \frac{1}{s} \right) - \bar{U}_p(\eta)' - \frac{V_1}{\eta} \bar{U}_p(\eta). \end{aligned}$$

Afterward, inserting the solution for displacement (14) into the dimensionless stress equations yields the stresses ($S = \sigma / (C_{11} E_b)$) in the hollow cylinder.

3 Results

In this study, closed-form solution for the transient thermal stress analysis of the functionally graded hollow cylinder subjected to periodic rotation and high-temperature difference is examined. It consisting of all metal inside (Ti-6Al-4V) and pure ceramic outside ($Z_r O_2$) is studied. The thermal and mechanical properties of these constituents are

Table 1 Material properties of ZrO_2 and Ti-6Al-4V [36]

Materials (W/(mK))	λ (GPa)	E	α (1/K)	ν	ρ (kg/m ³)	c_p (J/(kg.K))
Ti – 6Al – 4V	7.5	116.7	9.5×10^{-6}	1/3	4.43×10^3	560
ZrO_2	2.09	151	10×10^{-6}	1/3	5.5×10^3	418

Fig. 2 The motion of angular velocity over the time ($d=0.06$)

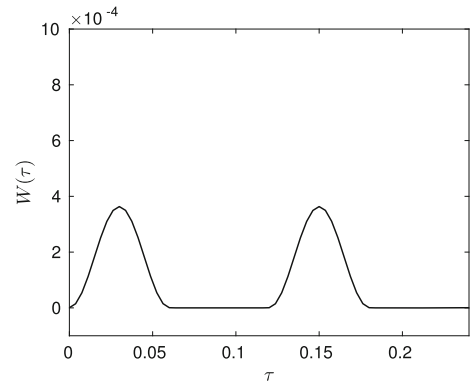


Table 2 Comparison of present study with PCM for temperature and displacement at dimensionless time $\tau = 0.034$

η	Θ		U	
	Present work	PCM	Present work	PCM
0.50	1.000706852	1.000706852	0.000990702	0.000990981
0.51	1.059674749	1.059674761	0.000989414	0.000989692
0.52	1.237377079	1.237377078	0.000987378	0.000987651
0.55	1.536464804	1.536464813	0.000989332	0.000989599
0.59	1.962369235	1.962369229	0.001001230	0.001001490
0.64	2.524639559	2.524639566	0.001028581	0.001028833
0.69	3.236465902	3.236465894	0.001075408	0.001075655
0.75	4.108035566	4.108035573	0.001143708	0.001143952
0.81	5.131087277	5.131087271	0.001232894	0.001233136
0.86	6.260507199	6.260507201	0.001338952	0.001339191
0.91	7.407707060	7.407707065	0.001453680	0.001453914
0.95	8.456038596	8.456038575	0.001564937	0.001565164
0.98	9.290589062	9.290589071	0.001658470	0.001658687
0.99	9.824119471	9.824119456	0.001720917	0.001721127
1.00	10.007068521	10.007068521	0.001742858	0.001743067

given in Table 1. Therefore, the inhomogeneity parameters corresponding to this pair of materials are $m_1 = -1.84$, $m_2 = 0.31$, $m_3 = -0.42$, $m_4 = 0.37$, and $m_5 = 0.074$. Note that, by changing the inhomogeneity coefficients (m_i , $i = 1, 2, 3, 4, 5$), results can be obtained for any pair of the materials.

It is assumed that inner radius, outer radius, angular velocity, ambient temperature, inner temperature, and outer temperature are $a = 0.5$, $b = 1$, $\omega = 50$, $T_0 = 20$, $T_a = 40$ ($\Theta_a = 1$), and $T_b = 220$ ($\Theta_b = 10$), respectively. Periodic angular velocity with period $2d$ ($d = 0.06$) is chosen as a partial function (3) with a sinusoidal load (Fig. 2).

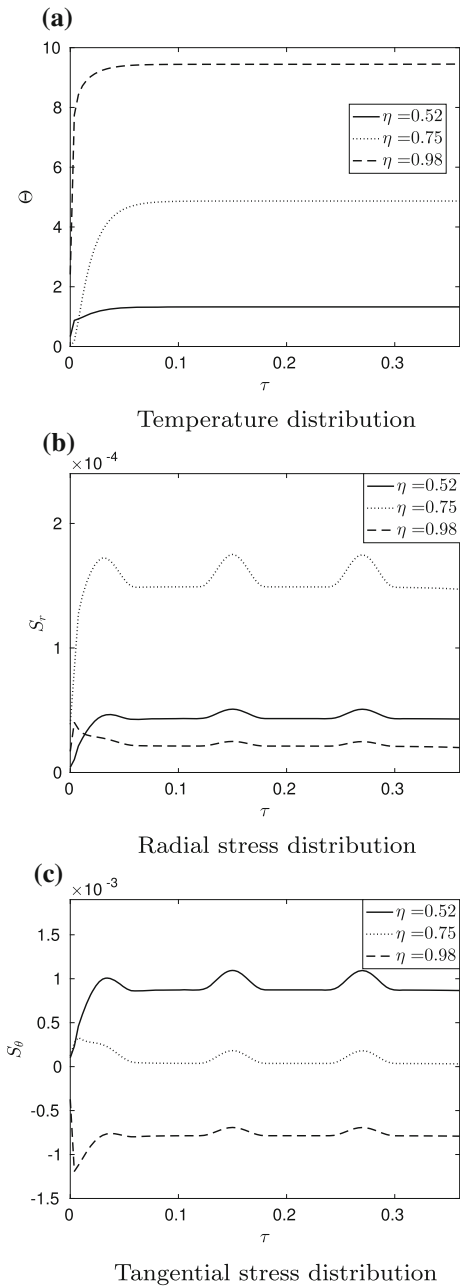


Fig. 3 Temperature and stress distribution over time at different points of the wall

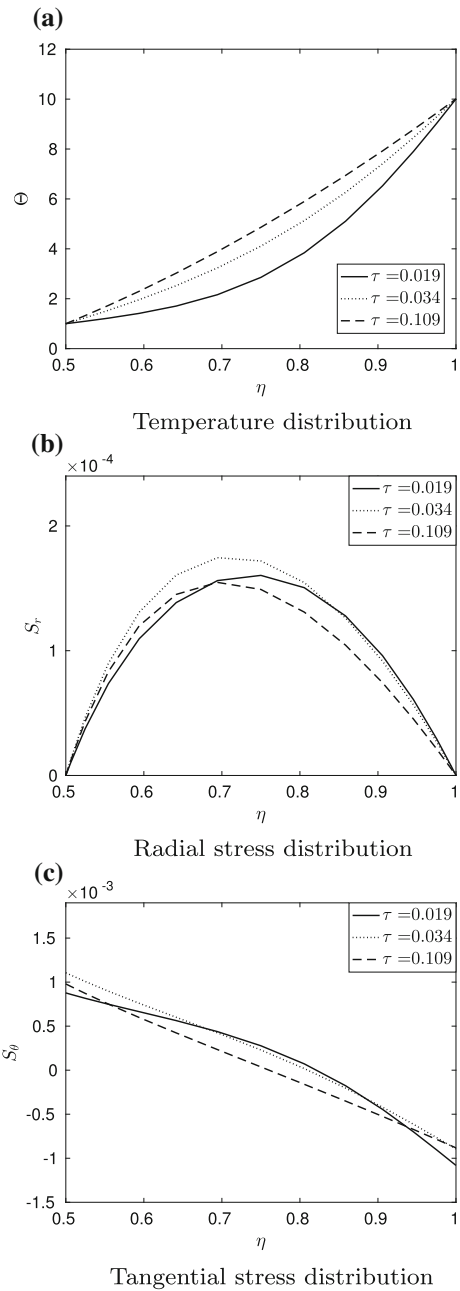


Fig. 4 Temperature and stress distributions across the wall for three different time periods

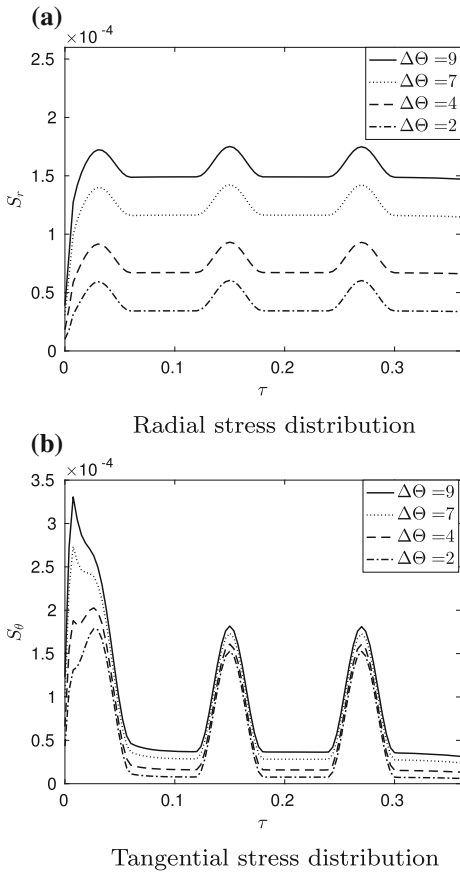


Fig. 5 The effects of temperature difference on stress distributions in the middle of the wall ($\eta = 0.75$)

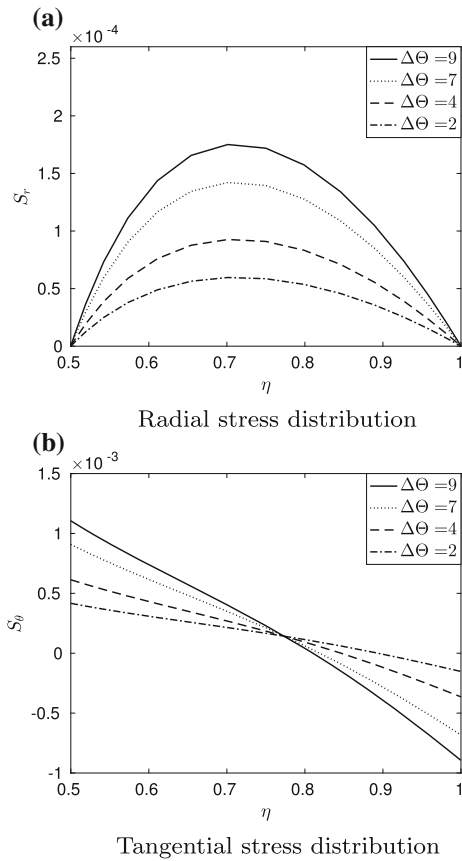


Fig. 6 The effects of temperature difference on stress distribution along the wall where the rotational effect is greatest ($\tau = 0.03$)

$$W(\tau) = \begin{cases} \sqrt{\frac{\rho_b b^2}{E_b}} \sin\left(\frac{\pi b^2}{\kappa d} \tau\right), & 0 \leq \tau \leq d, \\ 0, & d \leq \tau \leq 2d. \end{cases} \tag{18}$$

The Pseudospectral Chebyshev Method (PCM) based on the Chebyshev polynomial approach of the first kind is used to check the general solution obtained for temperature and displacement, see, e.g., Trefethen [37]. It simply provides a highly accurate approximation to the differentials by multiplying the differential matrix with the corresponding data vector. In this way, the solution is obtained by transforming the differential equation into a linear equation system. It is a commonly preferred method due to its high accuracy, low computational cost, and ease in implementation [38–40]. The general solution presented in this study and the pseudospectral Chebyshev solution are compared for fifteen points (fourteen intervals) in Table 2. It is observed that the results are consistent. The temperature and stress distributions over time at different points of the cylinder’s radial direction under both a periodic rotation effect and high temperature outside the cylinder are given in Fig. 3. The distribution of temperature (Fig. 3a), radial (Fig. 3b), and tangential stresses (Fig. 3c) over time are given, slightly inside the inner and outer walls of the cylinder and at the midpoint of the wall. In Fig. 3a, it is observed that the temperature increases towards the outer wall of the cylinder in accordance with the boundary condition. The effect of periodic rotation

and high-temperature difference on radial stress (Fig. 3b) due to traction-free boundary conditions on both walls is seen in the center of the wall. Unlike the radial stress, it is seen in Fig. 3c that the tangential stress magnitude increases from the outer wall to the inner wall.

The temperature and stress distributions along the wall for three different periods of time, before peak time ($\tau = 0.019$), at the peak time ($\tau = 0.034$), and the absence of the rotation ($\tau = 0.109$) are examined in Fig. 4. From Fig. 4a, it can be noticed that the temperature reaches a steady state and shows a linear distribution as time progresses. It is observed from Fig. 4b, c that when the effect of rotation is the highest ($\tau = 0.034$), the stresses take the highest values, and the stresses decrease when the rotation has no effect ($\tau = 0.109$).

Figures 5 and 6 illustrate the effects of temperature difference on stress distributions in terms of nondimensional time and radius at the presence of a periodic rotation. Note that in Figs. 5 and 6, $\Delta\Theta = \Theta_b - \Theta_a$. It is seen that the stresses increase as the temperature difference increases and, the effect of the tangential stress on the periodically rotating cylinder is greater than the stress in the radial direction.

Animations are created for temperature, radial, and tangential stresses to understand better the effect of periodic rotation and high-temperature difference on the hollow cylinder. The temperature distribution (Temperature.gif) exhibits a convex distribution in transient regime, while after a short dimensionless time (≈ 0.1 , see Fig 3a), it shows a linear distribution. Radial (Radial Stress.gif) and tangential (Tangential Stress.gif) stresses under the influence of constant, periodic angular velocity, and non-rotating states are affected by both rotation and temperature change. After the temperature distribution reaches the steady state, the stresses change only by the action of periodic rotation. Please see the online supplementary material.

4 Conclusions

This paper presents a closed-form solution to obtain transient temperature and stress distributions of functionally graded cylinder structural elements rotating at varying speeds. Transient temperature and stresses for a given ceramic–metal mixture are graphically presented under the influence of periodic rotation, high temperature, and the temperature gradient. The results obtained show that all parameters studied have a significant effect on stress distributions and temperature. With the closed-form solution presented in this article, it is possible to use the rotational speed acceleration to set new safe values for rotating structures and create higher and safer rotation speeds for steady-state operation. Besides, this solution can be adopted simply by changing the inhomogeneity coefficients in the power-law variation for any pair of materials.

References

1. Miyamoto Y, Kaysser WA, Rabin BH, Kawasaki A, Ford RG (1999) Functionally graded materials design, process and applications. Springer, New York
2. Kieback B, Neubrand A, Riedel H (2003) Processing techniques for functionally graded materials. *Mater Sci Eng A* 362(1):81–106
3. Shin KH, Natu H, Dutta D, Mazumder J (2003) A method for the design and fabrication of heterogeneous objects. *Mater Design* 24(5):339–353
4. Koizumi M (1997) FGM activities in Japan. *Compos Part B* 28(B):1–4
5. Akis T, Eraslan AN (2007) Exact solution of rotating FGM shaft problem in the elastoplastic state of stress. *Arch Appl Mech* 77:745–765
6. You LH, You XY, Zhang JJ, Li J (2007) On rotating circular disks with varying material properties. *J Appl Math Phys (ZAMP)* 58:1068–1084
7. Zenkour AM (2009) Stress distribution in rotating composite structures of functionally graded solid disks. *J Mater Process Technol* 209(7):3511–3517
8. Asghari M, Ghafoori E (2010) A three-dimensional elasticity solution for functionally graded rotating disks. *Compos Struct* 92(5):1092–1099
9. Nejad MZ, Rahimi GH (2010) Elastic analysis of FGM rotating cylindrical pressure vessels. *J Chin Inst Eng* 33(4):525–530
10. Peng XL, Li XF (2010) Thermal stress in rotating functionally graded hollow circular disks. *Compos Struct* 92(8):1896–1904
11. Rahimi GH, Arefi M, Khoshgoftar MJ (2011) Application and analysis of functionally graded piezoelectrical rotating cylinder as mechanical sensor subjected to pressure and thermal loads. *Appl Math Mech (Engl Ed)* 32(8):997–1008

12. Peng XL, Li XF (2012) Elastic analysis of rotating functionally graded polar orthotropic disks. *Int J Mech Sci* 60(1):84–91
13. Dai HL, Dai T, Zheng HY (2012) Stresses distributions in a rotating functionally graded piezoelectric hollow cylinder. *Meccanic* 47:423–436
14. Bayat M, Rahimi M, Saleem M, Mohazzab AH, Wudike I, Talebi H (2014) One-dimensional analysis for magneto-thermo-mechanical response in a functionally graded annular variable-thickness rotating disk. *Appl Math Modell* 38(19–20):4625–4639
15. Nejad MZ, Kashkoli MD (2014) Time-dependent thermo-creep analysis of rotating FGM thick-walled cylindrical pressure vessels under heat flux. *Int J Eng Sci* 82:222–237
16. Hosseini M, Dini A (2015) Magneto-thermo-elastic response of a rotating functionally graded cylinder. *Struct Eng Mech* 56(1):137–156
17. Jabbari M, Nejad MZ, Ghannad M (2015) Thermo-elastic analysis of axially functionally graded rotating thick cylindrical pressure vessels with variable thickness under mechanical loading. *Int J Eng Sci* 96:1–18
18. Gharibi M, Nejad MZ, Hadi M (2017) Elastic analysis of functionally graded rotating thick cylindrical pressure vessels with exponentially-varying properties using power series method of Frobenius. *J Comput Appl Mech* 48(1):89–98
19. Hosseini M, Dini A, Eftekhart M (2017) Strain gradient effects on the thermoelastic analysis of a functionally graded micro-rotating cylinder using generalized differential quadrature method. *Acta Mech* 228:1563–1580
20. Afshin A, Nejad MZ, Dastani K (2017) Transient thermoelastic analysis of FGM rotating thick cylindrical pressure vessels under arbitrary boundary and initial conditions. *J Comput Appl Mech* 48(1):15–26
21. Dai T, Dai HL (2017) Analysis of a rotating FGME circular disk with variable thickness under thermal environment. *Appl Math Modell* 45:900–924
22. Nematollahi MA, Dini A, Hosseini M (2019) Thermo-magnetic analysis of thick-walled spherical pressure vessels made of functionally graded materials. *Appl Math Mech (Engl Ed)* 40:751–766
23. Torabnia S, Aghajani S, Hemati M (2019) An analytical investigation of elastic–plastic deformation of FGM hollow rotors under a high centrifugal effect. *Int J Mech Mater Eng* 14(16):1–11
24. Yildirim S, Tutuncu N (2019) Effect of magneto-thermal loads on the rotational instability of heterogeneous rotors. *AIAA J* 57:2069–2074
25. Kacar I (2020) Exact elasticity solutions to rotating pressurized axisymmetric vessels made of functionally graded materials. *Mater Werkst* 51:1481–1492
26. Lin WF (2020) Elastic analysis for rotating functionally graded annular disk with exponentially-varying profile and properties. *Math Probl Eng* 2020:1–10
27. Bidgoli MO, Loghman A, Arefi M, Faegh RK (2020) Transient stress and deformation analysis of a shear deformable FG rotating cylindrical shell made of AL-SiC subjected to thermo-mechanical loading. *Aust J Mech Eng*. <https://doi.org/10.1080/14484846.2020.1842296>
28. Temesgen AG, Singh SB, Pankaj T (2020) Elastoplastic analysis in functionally graded thick-walled rotating transversely isotropic cylinder under a radial temperature gradient and uniform pressure. *Math Mech Solids* 26(1):5–17
29. Georgiades F (2018) Nonlinear dynamics of a spinning shaft with non-constant rotating speed. *Nonlinear Dyn* 93:89–118
30. Boukhalfa A (2014) Dynamic analysis of a spinning functionally graded material shaft by the p-version of the finite element method. *Latin Am J Solids Struct*. 11(11):2018–2038
31. Durbin F (1974) Numerical inversion of Laplace transforms: an efficient improvement to Dubner and Abate’s method. *Comput J* 17:371–376
32. Arpacı VS (1996) *Conduction heat transfer*. Addison-Wesley, Boston
33. Carslaw HS, Jaeger JC (1986) *Conduction of heat in solids*. Oxford University Press England, Oxford
34. Timoshenko SP, Goodier JN (1970) *Theory of elasticity*. McGraw-Hill Education United States, New York
35. Crandall SH, Dahl NC, Lardner TJ (1978) *An introduction to the mechanics of solids*. McGraw-Hill Publishing Company United States, New York
36. Yıldırım A, Yarımabaç D, Celebi K (2020) Transient thermal stress analysis of functionally graded annular fin with free base. *J Therm Stress* 43(9):1138–1149
37. Trefethen LN (2000) *Spectral methods in MATLAB*. SIAM, Philadelphia
38. Yarımabaç D (2019) A unified approach to hyperbolic heat conduction of the semi-infinite functionally graded body with a time-dependent laser heat source. *Iran J Sci Technol Trans Mech Eng* 43:729–737
39. Eker M, Yarımabaç D, Celebi K (2020) Elastic solutions based on the Mori–Tanaka scheme for pressurized functionally graded cylinder. *J Appl Math Comput Mech* 19(4):57–68
40. Eker M, Yarımabaç D, Celebi K (2021) Thermal stress analysis of functionally graded solid and hollow thick-walled structures with heat generation. *Eng Comput* 38(1):371–391